Patterns of Sedimentation from Surface Currents Generated by Turbulent Plumes

Mehran Zarrebini and Silvana S. S. Cardoso
Dept. of Chemical Engineering, University of Cambridge, Cambridge CB2 3RA, U.K.

A theoretical model was developed for the dynamics and deposition pattern from gravity currents generated by axisymmetric particle-laden plumes. This model incorporates the interaction between the particles in the environment and the continuing plume. This interaction plays a central role in the evolution of the behavior of the plume and on the sedimentation patterns on the surrounding floor. Theoretical predictions for the deposition patterns were successfully compared with data from laboratory experiments for environments of both infinite and finite lateral extent. The evolution of the particle concentration in the environment and in the surface current until steady state is attained was also examined. A simple analytical expression is proposed for the sedimentation rate on the ground in the case of dilute plumes. The application of these new results to estimate the patterns of sedimentation from industrial chimney emissions is also discussed.

Introduction

Particle-laden plumes and jets occur in many industrial, as well as environmental, processes. In industry, particle-laden flows have recently been used to improve heat transfer in fluidized bed heat exchangers. This technique is used, for example, with liquid nitrogen gasification systems: the frost layers that develop on the heat exchanger tubes reduce heat transfer and can cause an eventual failure of the system. The new technique utilizes a jet of solid particles which impinges onto the frost layers surrounding the heat exchange tubes causing continuous defrosting by abrading the ice formation (Schaflinger et al., 1997). The defrosting mechanism and surroundings of the flow have not yet been studied. It has also been recently suggested that impinging plumes and jets may allow the control of the nucleation step in precipitation processes. Here the fluid mechanics of the flow plays a central role on the rate of reaction. (Benet et al., 1999). Other examples of industrial plumes include gaseous emissions into the atmosphere and liquid effluents discharged into rivers and coastal waters, both of which normally contain very fine particles.

In the natural environment, particle laden plumes may be exemplified by hydrothermal flows at the bottom of the ocean, which introduce large amounts of fine metalliferous particles, dissolved chemicals, and heat into the ocean (Feely et al., 1987).

A significant number of theoretical and experimental studies have been carried out to investigate the behavior of particle-laden, turbulent plumes. Such work has been developed mainly in the context of geophysical flows. One of the most significant effects of particles is on the density and buoyancy of the plume. The addition of particles increases the bulk density of the fluid in comparison to the pure fluid. Thus, the emerging flow with particles has a diminished buoyancy flux. Carey et al. (1988) presented an experimental study on the phenomenological effects of particles on the fluid dynamical behavior of axisymmetric plumes. They found that plumes with small particle concentrations behave in accord with the theoretical models for one-phase plumes, with reduced buoyancy. However, as the particle concentration increases towards flows of neutral buoyancy, where the bulk density of the plume equals that of the environmental fluid, instabilities develop in the plume, which lead to partial collapse and to the generation of gravity currents. The experimental observations show that the particles assume a Gaussian profile of concentration about the plume axis. There is also some evidence that the radial spreading of particles is greater than

Correspondence concerning this article should be addressed to S. S. S. Cardoso.

that for momentum and that it is also dependent on the size of the particles. However, the available experimental data are not systematic, and no firm conclusion can be reached.

Plumes released in an environment of finite vertical extent, or in a density stratified environment such as the ocean or atmosphere, reach a maximum height. At this level, they spread out radially, forming a current. The sediment is suspended in the current by turbulence, but particles continuously settle out of the lower boundary of the current. Sparks et al. (1991) considered the sedimentation of particles from such gravity currents, both experimentally and theoretically. They showed that the accumulation of sediment on the ground follows a Gaussian distribution about the source. The authors noted that as the sediment settles out below the radially expanding current, it is drawn back towards the plume by a net inflow caused by the entrainment of ambient fluid at the plume margins, but this re-entrainment was not taken into account in their model. Such interaction between the particles in the environment and the plume has not been investigated theoretically or experimentally as yet. However, it will lead to much larger particle concentrations within the plume than expected considering the particles released at the source only, and will therefore play a central role in the evolution of the behavior of the plume and on the sedimentation patterns on the surrounding floor.

In this article, we present a model that describes the dynamics and deposition pattern of radially spreading gravity currents generated by particle-laden plumes. The particles are assumed to be sufficiently small that they settle with their Stokes velocity. We consider the re-entrainment of particles into the plume from the surrounding sedimenting veil.

Predictions of deposition patterns from the model are successfully compared with new data from laboratory experiments and with previous data by Sparks et al. (1991). Experimental and theoretical predictions for the particle concentration profiles in the environment and in the plume are also presented. Environments of both infinite and finite lateral extent are considered. Finally, a simple analytical expression is proposed for the sedimentation profile on the ground in the case of dilute plumes. It is discussed how these new results may be used to estimate the patterns of sedimentation from industrial chimney emissions.

Experimental Procedure

The experiments were conducted in a tank of cross section 75 cm $\times$ 75 cm and height 75 cm. The tank was filled to a depth of 30 cm with a uniform NaCl solution of approximately 3%(w:w). The accurate concentration of this solution was measured by refractometry. A mixture of fresh water and particles, contained in a bucket of a 10 L volume was stirred continuously to achieve a uniform suspension during an experiment. Particle concentrations ranged from 5 to 6 g/L. The mixture was pumped continuously through a 7-mm dia nozzle positioned at the center of the base of the tank (Figure 1). The flow rate into the tank was controlled by a flow diverter; the remainder of the flow was recycled back into the bucket, aiding mixing of the suspension in the bucket. The flow rate was measured by timing the decrease in the level of the suspension in the bucket. The flow rates used varied between 5.6 and 13.5 cm^3/s; these are sufficiently small for the flow to approximate that of a pure plume at a short distance above the source. The volume of suspension injected into the tank during each experiment resulted in an increase of approximately 3% in the level of liquid in the tank. The effect of this change on the flow in the plume and surroundings is sufficiently small to be neglected in our modeling section.

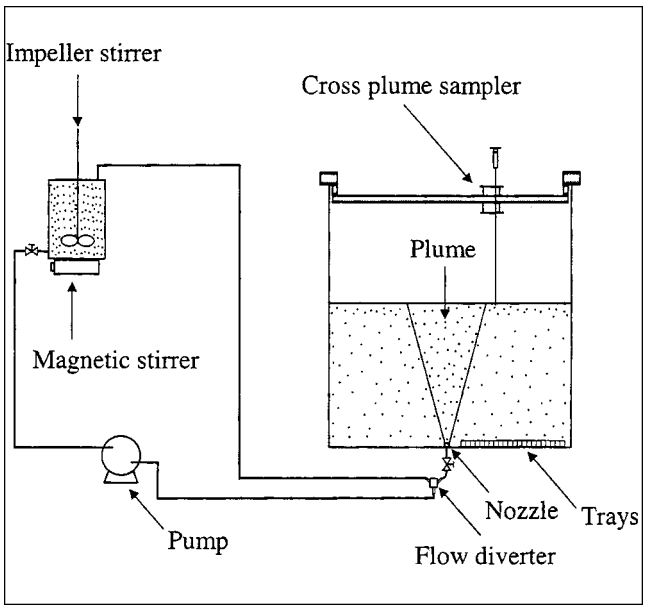

Figure 1. Experimental apparatus.

The particles used in all experiments were sieved fractions of ballotini with a density of 2.47 g/cm^3. The particle-size distribution in each fraction was determined using a Coulter counter, which works on the electrical sensing zone method (Allen, 1997). The fractions were regarded as approximately monodisperse. As the Stokes particle settling velocities are proportional to the square of the diameter of the particle, the root-mean square diameter was used to characterize each particle fraction. The root-mean square diameters of the particle fractions used ranged between 50 and 80 μm. The experimental conditions for each run are summarized in Table 1.

Figure 2 shows a sequence of photographs of the particle-laden plume rising in the tank of salty water. In the first photograph, we see that as the plume rises, it dilutes with in-

Table 1. Experimental Conditions

Exp.	Flow Rate Q_0 (cm^3/s)	Buoyancy Flux B_0 (cm^4/s^3)	Particle Dia. d_p (μm)	Duration of Exp.(s)	Ambient Dens. ρ_e (g/cm^3)	Particle Conc. at Source C_{p0} (g/L)
11b	6.41	111.4	49.28	900	1.0211	5.00
12a	13.24	203.4	74.38	506	1.0203	6.00
13	13.52	236.1	65.03	476	1.0225	6.00
14a	11.93	183.2	80.70	540	1.0203	6.00
14b	7.49	115.0	80.70	770	1.0207	6.00
15a	5.62	109.5	50.37	924	1.0246	6.00
16	12.86	215.8	73.03	476	1.0218	6.00

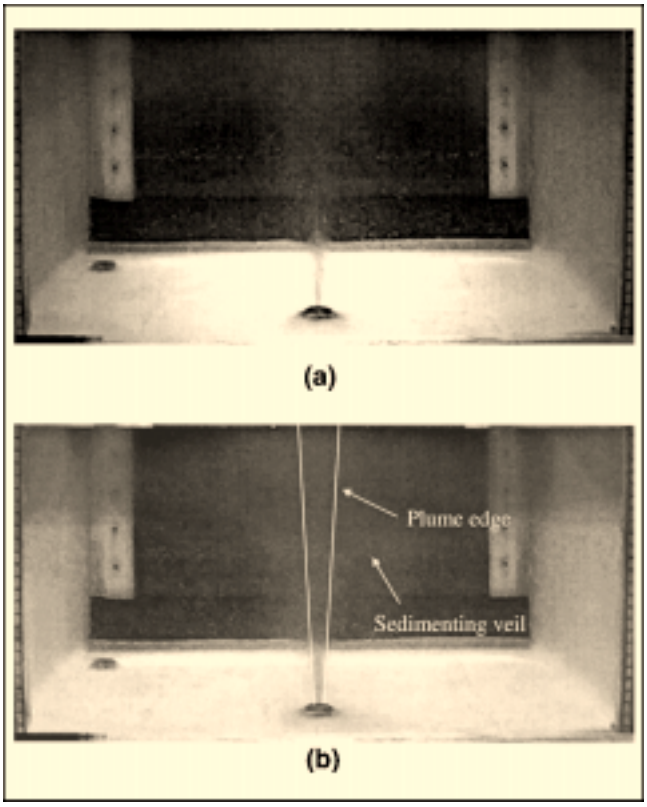

Figure 2. Sequence of an experiment at times (a) 1 min and (b) 7 min.

creasing distance from the source due to entrainment of the surroundings. The plume appeared to be fully turbulent and the Reynolds number was of the order of 2,500. In such a plume, the magnitude of root-mean-square turbulent fluctuations in vertical velocity are typically 24% of the vertical time-averaged velocity, that is, of the order 2 cm/s at the plume axis; the radial velocity fluctuations are typically 0.75 cm/s at the plume axis (Papanicolaou and List, 1988). The widths of the root-mean-square vertical and radial velocity profiles scale with height in the plume and are approximately equal to $1.3b$ (Papanicolaou and List, 1988), with b being the effective radius of the plume as defined in the following section; this corresponds to approximately 5–7 cm at a height of 30 cm above the nozzle, and is in accord with our experimental observations.

Upon reaching the free surface, a current is produced which spreads radially outward. The Reynolds number of the current was of the order of 600, corresponding to turbulent flow (Manins 1973, 1979). In such a current, the turbulent vertical velocity fluctuations are able to keep the particles in suspension; we estimate that the vertical root-mean-square velocities were of the order of 2 cm/s through direct observation, while the particle Stokes velocities were in the range 0.2–0.6 cm/s. The thickness of the current at small radial positions was typically 5 cm.

Initially, the environment is one of pure fluid. However, with time, particles settle from the base of the surface current and produce a veil around the plume. This veil of particle-laden fluid slopes radially inward towards the plume, where a fraction of the particles are incorporated into the plume. This phenomenon can be seen in Figure 2b which was taken approximately seven min after the start of the experiment. The two continuous white lines depict the plume edge and the hazy cloud surrounding the plume is the veil of particle-laden fluid.

A number of trays were positioned radially away from the nozzle on the floor of the tank in order to collect the sedimenting particles. Each tray had a cross section of 1.9 cm $\times$ 1.9 cm. At the end of an experiment, the particles were extracted from each tray using a syringe and placed in vials for analysis. The diameter of the sampling syringe was 0.15 cm. The concentration of particles was determined using the Coulter counter.

In a few experiments, the gravity current and the environment were sampled. The syringe was used to extract samples of 5 cm^3 of suspension at different radial and vertical positions. Each sample was withdrawn slowly and steadily over about 10–15 s so that the fluid was withdrawn from a location close to the needle entrance. This strategy also allowed us to overcome the difficulty of sampling the turbulent, and, hence, highly time-dependent, flows in the plume and gravity current; each sample represents an average over a time interval that is sufficiently long to capture a number of turbulent fluctuations, and is sufficiently short that the long-time evolution of the concentration can still be followed (see Results and Discussion).

Theory

Environment of infinite lateral extent

Consider a turbulent, axisymmetric particle-laden plume created by the release of a buoyant suspension in a body of liquid of depth H. We assume that the density of the environment is greater than that of the suspension owing to a thermal or compositional difference; for simplicity, we shall describe here the environment as consisting of an aqueous solution of salt. The turbulent plume entrains surrounding ambient fluid as it rises and, hence, its bulk density is the local volume average of the density of the particles and the density of the interstitial fluid, consisting of water and salt, given by

$$\rho = \rho_w + 0.6954C_s + C_p \qquad (1)$$

where ρ_w is the density of water, and C_s and C_p are the concentrations of salt and of particles, respectively, expressed in mass per unit volume of mixture. Equation 1 was obtained using data for aqueous NaCl solutions from Weast (1971).

The plume rises to the surface of the liquid and spreads out radially producing a surface current, as shown in Figure 3. The particles in suspension settle across the bottom viscous sublayer of the surface current with their Stokes free fall velocity u_{st} (Martin and Nokes, 1988; Sparks et al., 1991). These particles are drawn back towards the buoyant plume by the net inflow caused by entrainment below the spreading level. As a result, a fraction of the particles are re-entrained into the plume, while the rest of the particles deposit on the floor. Owing to this continuous variation of the concentration

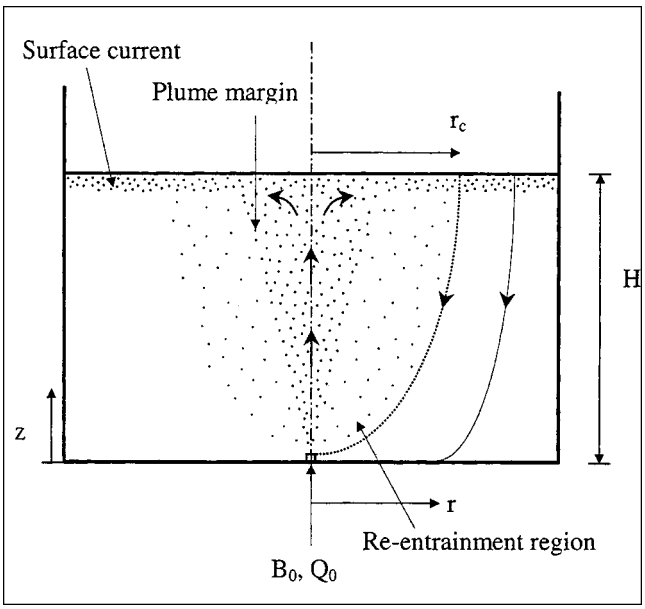

Figure 3. Trajectories of the particles released from the surface current.

of particles in the ambient, the behavior of the plume is time-dependent. However, in this article we are interested in the ultimate steady-state behavior of the system. Thus, the equations expressing conservation of volume, momentum, particles and buoyancy for the plume are, respectively

$$\frac{d}{dz}(wb^2) = 2\alpha bw \tag{2}$$

$$\frac{d}{dz}(w^2b^2) = b^2 g\frac{\rho_e - \rho}{\rho_r} \tag{3}$$

$$\frac{d}{dz}\left[wb^2(C_s - C_{se})\right] = -b^2 w\frac{\partial C_{se}}{\partial z} \tag{4}$$

$$\frac{d}{dz}\left[wb^2(C_p - C_{pe})\right] = -b^2 w\frac{\partial C_{pe}}{\partial z} \tag{5}$$

where z denotes the vertical co-ordinate, increasing upward, with its origin at the source; w is the plume velocity; b is the plume radius; ρ_e is the ambient density; ρ_r is the reference density taken to be equal to the initial ambient density; and C_{se} and C_{pe} are the concentration of salt and the concentration of particles in the environment at the edge of the plume, respectively. It is usually assumed that the mean inflow velocity across the edge of the plume is proportional to the local mean upward velocity in the plume, and we invoke this assumption in this article; the constant of proportionality, the entrainment constant, is $\alpha = 0.125$ (List, 1982; Turner, 1986). This is a very powerful similarity assumption, which implies the same kind of turbulent structure and balance of forces at each height. Top hat profiles of equal width have been assumed for the vertical velocity, and for the particle and buoyancy distributions in the plume; the exact analytic form chosen for these profiles does not affect our conclusions since all the results are expressed in terms of mean values, averaged with respect to the volume flux in the plume. We neglect the sedimentation of particles at the margins of the turbulent plume. This approximation is valid for sufficiently small particles and large plume buoyancy fluxes (Ernst et al., 1996). Equations similar to Eqs. 2–5 were originally derived by Morton et al. (1956) for a one-phase plume and have been discussed in detail elsewhere (Turner, 1979).

The particle concentration varies along the surface current due to advection and settling. We assume that the Reynolds number of the current is sufficiently large that turbulent mixing maintains a vertically uniform particle concentration in the current, without any detrainment of particle-free fluid at the top of the current. Then, a particle mass balance in the radially expanding current leads to

$$C_p(r_s) = C_{ps}\exp\left[-\frac{u_{st}}{Q_s}\pi\left(r_s^2 - b_s^2\right)\right] \tag{6}$$

where r_s denotes the radial position along the surface current, Q_s is the volumetric flow rate of the plume at the free surface, b_s is the radius of the plume at the free surface, and C_{ps} is the concentration of particles in the plume at b_s. Here, we have assumed that the volumetric flow lost by sedimentation from the surface current is negligible. The effect of particle concentration on the settling velocities of the particles is also assumed negligible.

We shall use a Lagrangian approach to follow the motion of the particles in the environment. The path of a particular particle depends on the radial position at which it leaves the surface current (see Figure 3). Particles falling out of the surface current at small radii tend to be re-entrained into the plume, while particles falling out at larger radial positions settle on the ground. A critical radius r_c separating these two regions may be defined: a particle settling from the current at r_c has a trajectory which brings it back to the source of the plume, so that it is re-entrained (Sparks et al., 1991). In general, the trajectory of a particle is described by

$$\frac{dz}{dt} = -u_{st} \tag{7a}$$

$$\frac{dr}{dt} = u_e = -\frac{b}{r}\alpha w \tag{7b}$$

where u_e is the radial inward velocity of the environmental fluid. The thickness of the surface current is typically small compared to the vertical extent of the environment below, and we shall therefore assume that particles leave the surface current at height H.

In steady state, the flow rate of particles in the surface current at the critical radius is equal to the flow rate of particles at the plume source

$$Q_0 C_{p0} = Q_s C_p\,|_{\text{critical radius}} \tag{8}$$

where Q_0 is volumetric flow rate at the source and C_{p0} is the particle concentration at the source. We now need to obtain the field of particle concentrations surrounding the plume

from the Lagrangian description above. The particles in the environmental fluid that is re-entrained into the plume at height z_f originated from the surface current at radial position r_s, and thus continuity requires that the concentration of particles in the ambient at the edge of the plume satisfies

$$C_p(z_f) = \frac{C_p(r_s)u_{st}r_s}{b\alpha w}\cos^2\beta\frac{dr_s}{dz_f} \tag{9}$$

where $\beta = \arctan(u_{st}/\alpha w)$. Conservation of the mass of particles between the surface current and the floor leads to an expression for the concentration of particles settling on the floor at radial position r_f

$$C_p(r_f) = \frac{C_p(r_s)r_s}{r_f}\frac{dr_s}{dr_f} \tag{10}$$

The boundary conditions for Eqs. 2–5 specify the plume flow rates of volume, momentum, particles and buoyancy at the source, respectively

$$\pi b^2 w = Q_0 \tag{11a}$$

$$\pi b^2 w^2 = M_0 \tag{11b}$$

at $z = 0$

$$\pi b^2 w C_p = Q_0 C_{p0} \tag{11c}$$

$$\pi b^2 w\left[(C_{se} - C_{s0}) + (C_{p0} - C_{pe})\right] = B_0 \tag{11d}$$

Equations 1–11 were solved numerically after a suitable change of variables, using *Mathematica*.

The mass-flow rate of particles depositing on the floor per unit radial distance is then

$$F(r_f) = 2\pi r_f C_p(r_f)u_{st} \tag{12}$$

Simplified model for dilute plumes in an infinite environment

If the concentration of particles in the source suspension is small, then the motion of the plume is controlled by the buoyancy due to salinity. The density changes in the environment due to the presence of particles may then be neglected, and the plume behaves as if rising in a uniform environment. For such conditions, we may simplify the analysis presented in the previous subsection. Quantitatively, a particle-laden plume may be considered dilute when

$$\frac{H}{\rho_r - \rho_0}\frac{d\rho_e}{dz} \ll 1 \tag{13}$$

at all depths.

The model Eqs. 1–11 may then be solved analytically. The volumetric flow rate and the concentration of particles in the plume at the spreading level are given by, respectively

$$Q_s = \frac{6}{5}\alpha\pi\left(\frac{9}{10}\alpha B_0\right)^{1/3}H^{5/3} \tag{14}$$

$$C_{ps} = \frac{Q_0 C_{p0}}{Q_s}\exp(1) \tag{15}$$

The concentration profile in the gravity current may be obtained by substituting Eqs. 14 and 15 into Eq. 6. Using the result in Eq. 10 leads to the following expression for the mass flux of particles depositing on the floor

$$F(r_f) = 2\pi r_f u_{st} C_{ps}\exp\left[-\frac{u_{st}}{Q_s}\pi\left(r_f^2 - b_s^2 + \frac{Q_s}{\pi u_{st}}\right)\right] \tag{16}$$

Environment of finite lateral extent

Consider now a plume rising in a region of finite lateral extent, say with cross-sectional area $A = \pi R^2$, where R is an equivalent radius. In this case, the entrainment into the plume causes the environmental liquid surrounding the plume to move downward. If the density difference between the surface current and the liquid just beneath it is sufficiently large, then the downward motion may be approximately described by a uniform velocity U. Continuity is thus written as

$$-\pi R^2 U = \pi b^2 w \tag{17}$$

where it has been assumed that $R^2 \gg b^2$.

The first plume fluid that spreads at the surface is less salty than the environmental fluid below it and, hence, a concentration discontinuity is produced—the first front (Baines and Turner, 1969). As this less dense fluid moves downward and is re-entrained into the plume, new plume fluid arrives at the top in an even less dense condition. As a result, a stable salt concentration distribution is built up, gradually filling the original uniform environment. Owing to this continuous variation of the ambient properties, the behavior of the plume is time-dependent and no steady state is achieved. However, if the aspect ratio R/H is large for all times, then the time rates of change of the plume properties can be shown to be sufficiently small to be neglected in the relevant conservation equations (Manins, 1973). The plume is then of small radius compared to R, and the ambient behaves quasi-steadily as far as the plume is concerned. Equations 2–5, describing the plume, are then still valid.

The salt concentration field in the environment is governed by

$$\frac{\partial C_s}{\partial t} = -U\frac{\partial C_s}{\partial z} \tag{18}$$

Molecular diffusion and mixing have been neglected here.

At the bottom of the radially spreading surface current, the liquid now moves downward with velocity U_s and the particles settle from the current with vertical velocity $U_s + u_{st}$. A particle mass balance on the surface current, taking into account this radial decrease of volumetric flow rate, yields

$$C_p = C_{ps}\left[1 - \frac{U_s}{Q_s}\pi\left(r^2 - b_s^2\right)\right]^{u_{st}/U_s} = C_{ps}\left[\frac{R^2 - r^2}{R^2 - b_s^2}\right]^{u_{st}/U_s} \tag{19}$$

The trajectory of a particle leaving the surface current is now described by

$$\frac{dz}{dt} = -\left(u_{st} + U\right) \tag{20a}$$

$$\frac{dr}{dt} = u_e = -\frac{b}{r}\alpha w \tag{20b}$$

Equations 1–5, 8–12, and 18–20 describe the motion of a particle-laden plume in an environment of finite lateral extent. This system of equations was solved numerically.

In the next section, we present and compare the predictions of the three models developed above.

Results and Discussion

In this section, we compare our theoretical predictions with new experimental results, obtained as described earlier, and with experimental data of Sparks et al. (1991) and Carey et al. (1988). The novel contribution of present work lies on the effects arising from the re-entrainment of particles from the environment into the plume. We demonstrate below that this interaction is non-negligible and affects the transport of particles in the plume and gravity current, as well as the particle concentrations in the environment and the ultimate deposition pattern on the ground.

Our theory and experiments concern a source with constant concentration of particles. However, in the experiments of Sparks et al. (1991) and Carey et al. (1988), the particle concentration in the source suspension decreased exponentially with time, as particle-laden fluid was discharged and progressively replaced by fresh water. Nevertheless, as the time scale for the variation of the concentration in the source suspension $\tau = V/Q \sim 1{,}000$ s is very much larger than the time scale for steady state of the flow in the tank $\tau = H/u_{st} \sim 100$ s, we shall assume that a quasi-steady state was achieved in the experiments of those authors; here, V denotes the volume of the bucket containing the suspension of particles. We may, therefore, compare our predictions with the experimental results of those authors.

Figure 4 shows the nondimensional rate of accumulation of sediment on the tank floor as a function of radial distance. The experimental results display a well-defined maximum, beyond which the particle flux decreases with increasing radial position. We note that this maximum arises as a result of the exponential decrease in concentration with radial distance in the gravity current (Eq. 6) and the linear increase of the area of the differential annulus for deposition, expressed in Eq. 12. Figure 4 shows excellent agreement between the experimental data and the theoretical prediction for an infinite environment as discussed earlier. There is a significant deviation at large radial positions for experiment 14a listed in the figure. This difference is attributed to the effect of the tank wall.

In Figure 5, we compare the predictions of the three theoretical models. The solid and dashed lines represent the numerical solution for an infinite an a finite environment, respectively. For the experimental conditions studied, the difference between the deposition pattern for a finite and an infinite environment is relatively small and within the accuracy of the experimental data. We also show the prediction of the simplified model for dilute plumes as a dotted line. It may be concluded that for the low concentrations of particles used in our experiments, the assumption of dilute plume behavior is valid.

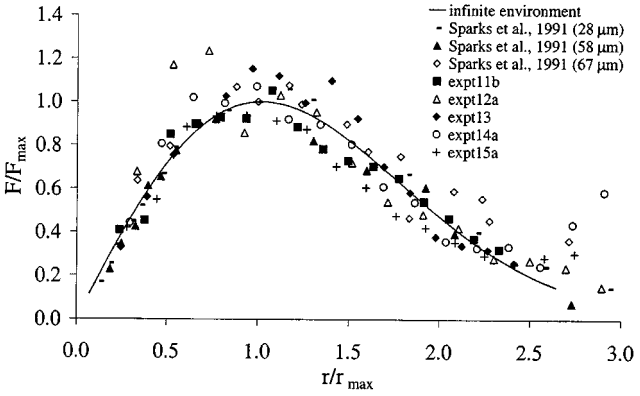

Figure 4. Nondimentional rate of accumulation of sediment on the tank floor per unit radial distance as a function of radial position.

In Figure 6, we show the predictions of the three theoretical models for $C_{p0} = 15$ g/L, $\rho_e = 1.15$ g/cm^3 and $Q_0 = 13.5$ cm^3/s. For such a large particle concentration and large buoyancy flux, the effects of a finite size tank and of the presence of particles in the plume become significant. In a finite environment, the downward advection of the ambient fluid leads to a larger particle flux and the maximum in the deposition rate lies closer to the source. For large particle concentrations, the re-entrainment of particles into the plume results in a significant reduction of the buoyancy of the plume, and, consequently, the simplified model underpredicts the rate of deposition of particles. For such situations, only the most detailed model, that of a finite environment, would describe the flow in the tank accurately. As we shall be comparing our theory with the experimental data of Sparks et al.

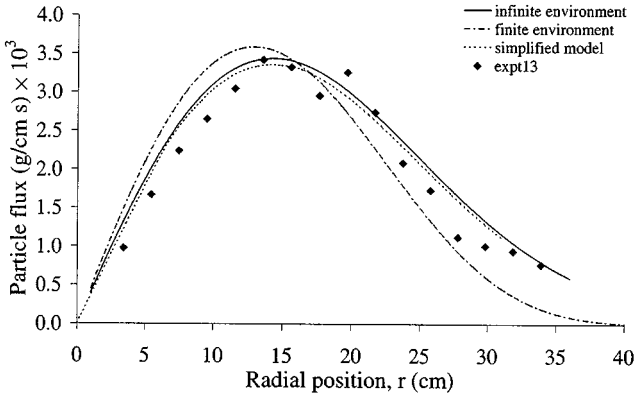

Figure 5. Predictions of the three theoretical models for experiment 13.

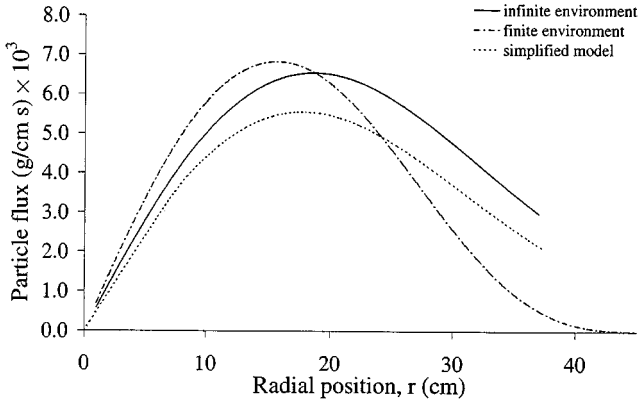

Figure 6. Predictions of the three theoretical models for a plume with large buoyancy flux, $B_0 = 1{,}660$ cm^4/s^3, and large particle concentration $C_{p0} = 15$ g/L.

(1991) and Carey et al. (1988), who used relatively high particle concentrations in the source suspension, but small buoyancy fluxes, we shall mainly use the predictions of the model for an infinite environment in the following discussion.

Figure 7 shows experimental data and theoretical predictions for the particle concentration profile along the surface current. Samples of the current at several radial positions were taken at three different times. We plot two theoretical curves for the concentration profile, one corresponding to the moment the plume fluid first spreads out at the surface, denoted "initial," and the other corresponding to steady state. The particle concentration in the current decays exponentially with radial position, as predicted by Eq. 6. We may see that the concentration of particles at small radial positions increases with time. This effect is a consequence of the re-entrainment of particles from the sedimenting veil into the plume. The experimental data is well contained between the two theoretical bounds and tends to the steady-state predictions at larger times. The agreement between the experiments and theory is very good, except at positions further away from the plume, where the concentration of particles is very low. At such low particle concentrations, the measurements are not accurate.

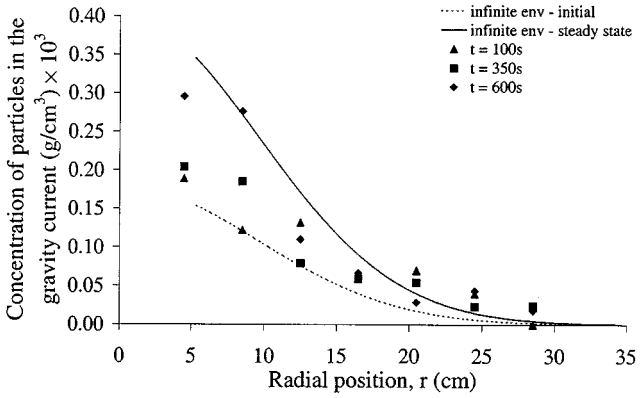

Figure 7. Evolution of the particle concentration profile in the surface current for experiment 14b.

Figure 8 shows the vertical concentration profile of particles in the environment at a radial position of 13.5 cm. Experimental data for three different times are presented. The concentration of particles increases with time and approaches a steady-state profile. At steady state, the concentration of particles increases with increasing height in the tank. Such a profile is a consequence of the radial inward motion of particles and fluid. The trend of increasing particle concentration with height is in good agreement with our theoretical prediction. Such a spatial distribution of particles results in an unstable density profile in the sedimenting veil. This seems to be at the origin of the thin fingers of particle-rich fluid, which could be seen moving downward in the sedimenting veil in some of our experiments. However, the motion associated with these finger-like structures does not seem to have affected the deposition patterns in our experiments. The effects of such instability will, however, become more important at higher particle concentrations, as the length scale and growth rate of the Rayleigh-Taylor instability will increase. This will be the subject of a future study.

In Figure 9, we compare our theoretical predictions for the particle concentration profile across the sedimenting veil with experimental data from Carey et al. (1988). Data for two different heights are presented. The particle concentration in the veil around the plume decays with radial position, in accord with the theory. Once more, we note that due to the relatively small particle concentrations in the veil, it is difficult to obtain accurate measurements. We also show the predicted top hat concentration in the plume and the corresponding Gaussian distribution

$$C_p = C_{pc} \exp\left(-\frac{r^2}{b_G^2}\right) \tag{21}$$

where the Gaussian plume radius is $b_G = b/\sqrt{2}$ and C_{pc} is the concentration of particles at the plume axis. While the theory using a Gaussian profile in the plume predicts a discontinuity in the concentration of particles at the edge of the plume, the experimental data show a continuous decrease in

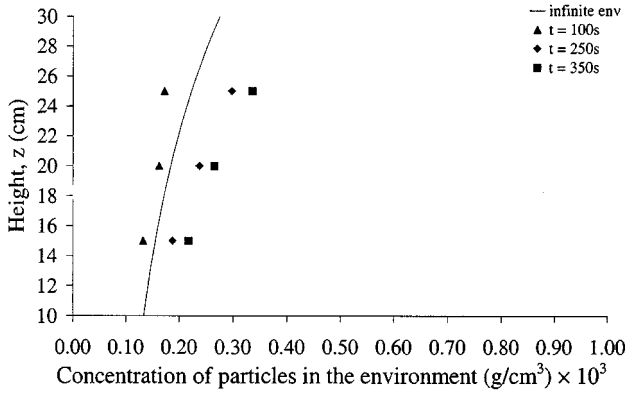

Figure 8. Evolution of the particle concentration profile in the environment at radial position 13.5 cm for experiment 16.

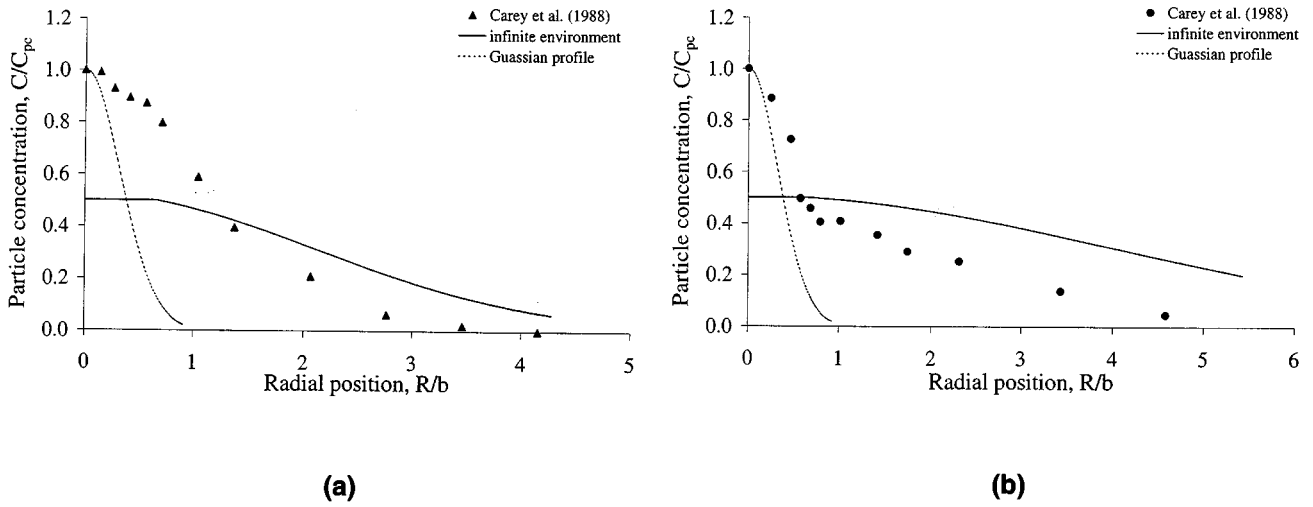

Figure 9. Particle concentration profile across the plume and the sedimenting veil at heights (a) 15 cm and (b) 30 cm.

concentration. We believe this is a result of the complex flow pattern at the edge of the turbulent plume, where eddies continuously engulf and mix fluid and particles. Our model does not capture the detail of such behavior. The concentrations in the plume are substantially greater than expected if the plume entrained pure ambient fluid, as noted previously by Carey et al. (1988). Quantitatively, Eq. 15 indicates that, in steady state, the concentration of particles in the plume at the spreading level is 2.7 times that expected if the plume entrained pure ambient fluid.

Application of the Model to Industrial Gaseous Emissions

We shall now consider the quantitative application of the model developed in this article to the discharge into the atmosphere of particle-laden gas from a typical combined gas turbine plant and a typical boiler or furnace on a process plant. These releases generally occur on many large process plants, where power and steam are consumed and produced.

Our model is directly applicable to incompressible fluids. In the examples above, the vertical extent of motion in the atmosphere will be such that it is not possible to treat air as an incompressible gas. However, the analysis may still be applied to the atmosphere by replacing absolute temperatures and densities for potential temperatures and potential densities (Tritton, 1988).

In a density stratified environment, such as the atmosphere, the buoyancy flux in the plume decreases with height and the plume eventually spreads out at the level at which the density in the plume equals that in the atmosphere (the level of neutral buoyancy). An equation for the height of rise of a plume in a linearly stratified environment was originally derived by Morton et al. (1956) from a momentum, buoyancy, and mass balance; uncertainties about the multiplying constant were later removed by a direct experiment (Briggs, 1969). In a still atmosphere with a positive, constant gradient of potential temperature in the vertical direction, the particle-laden, hot gas will rise to a height H given by (Turner, 1979)

$$H = 3.76 B_0^{1/4} N^{-3/4} \tag{22}$$

Here N is the buoyancy frequency, a measure of the strength of the stratification, defined as

$$N = \left(-g \frac{1}{\rho} \frac{d\rho}{dz} \right)^{1/2} = \left[g \frac{\Gamma}{T_r} \left(1 + \frac{\frac{dT}{dz}}{\Gamma} \right) \right]^{1/2} \tag{23}$$

where T_r is the absolute temperature at the source level and Γ is the adiabatic temperature gradient. It must be stressed that Eq. 22 applies to a still atmosphere. If there is wind, the plume will be carried away and will have suffered more entrainment by the time a given height is reached (Morton et al., 1956). Thus, the estimated heights will be too great under windy conditions, but the magnitude of this effect will not be considered at present.

We shall consider a standard atmosphere for which $T_r = 288$ K, $\Gamma = 9.8$ K/km, and the rate of decrease of temperature with height is 6.5 K/km (Morton et al., 1956). Thus, $N = 0.02$ s^{-1}. We shall see that, in the examples under study, the buoyancy flux at the source is mainly due to the difference between the source temperature and the atmospheric tem-

Table 2. Typical Data for Gaseous Emissions from a Combined Gas Turbine and a Boiler (Staples, 1997)

	Turbine	Boiler
Height of stack (m)	50	70
Diameter of stack (m)	5	1.5
Exit velocity (m/s)	18	15
Exit temperature (K)	398	523
Particulate emission rate (g/s)	1	1

perature, as the particle concentration is so small that its contribution to the density of the plume is negligible. Hence

$$B_0 = g\beta(T_0 - T_r)Q_0 \tag{24}$$

where T_0 is the source temperature and $\beta = 1/T_r$ is the thermal expansion coefficient of air.

We may now apply our model to predict the pattern of deposition of particles in the atmosphere surrounding the source and at ground level. The emission data used are presented in Table 2. We assume the particulate pollutant consists of ash particles of diameter 30 μm and a density of 1.5 g/cm^3. Once the height of rise in the atmosphere is calculated from Eq. 22, we shall use the simplified model and thus neglect the effect of stratification on the plume behavior. This simple analysis is supported by the observation that, up to 80% of its maximum height, the plume behavior is little different from that in a uniform environment (Turner, 1979) and will suffice to illustrate the behavior of the two releases in a still atmosphere.

For the boiler, Eq. 22 predicts that the smoke will rise to about 270 m above the source. At this level, the flow rate in the plume is approximately 7,000 m^3/s and the plume spreads out radially forming a gravity current. Figure 10a shows the predicted flux and concentration of particles at ground level. There is a pronounced maximum in the accumulation per unit distance at approximately 170 m from the source. The maximum concentration occurs near the source and is just above 1×10^{-7} kg/m^3. For the turbine example, the flow rate of gas released into the atmosphere is much larger and, hence, in spite of the lower exit temperature, the plume attains a height of 400 m. The flow rate of the plume at this level is 30,000 m^3/s. Figure 10b shows the predicted flux and concentration of particles at ground level. There is a pronounced maximum in the accumulation per unit distance at approximately 350 m from the source. The maximum concentration occurs near the source and is just above 3×10^{-8} kg/m^3. The higher concentration levels at the ground in the case of the boiler release are a result of the lower buoyancy flux at the source and, hence, a lower dilution of the original emission as it rises in the atmosphere. In both examples, smaller particles would be transported to larger distances away from the source.

Conclusions

We have presented a numerical model for the dynamics and deposition pattern of radially spreading gravity currents generated by axisymmetric particle-laden plumes. Our model takes into account the interaction between the plume and the particles sedimenting in the environment surrounding the plume. As a result of the re-entrainment of particles from the environment into the plume, the concentrations within the plume can reach 2.7 times those expected if the plume entrained pure ambient fluid.

Our theoretical predictions for the deposition patterns on the floor were successfully compared with data from laboratory experiments. The rate of accumulation of sediment per unit radial distance exhibits a well-defined maximum, beyond which particle flux decreases away from the source. In a finite environment, the downward advection of the ambient fluid leads to a larger particle flux and the maximum in the deposition rate lies closer to the source.

We also examined the evolution of the concentration of particles in the surface current and in the environment until steady state was attained. It was found that the steady-state particle distribution in the sedimenting veil results in an unstable density stratification, which is at the origin of the formation of a finger-like convective instability.

Finally, we considered the limit case where the concentration of particles at the source is sufficiently small that the motion of the plume is completely determined by the concentration of the agent producing the buoyancy and not the particles. For such dilute plumes, a simple analytical expression for the sedimentation profile on the ground was derived.

We applied our new model to estimate the patterns of sedimentation from industrial particulate emissions. Both a typical combined gas turbine plant and a boiler were considered. It was found that the smoke plumes arising from these sources ascend in a still atmosphere to a typical height of 300–400 m. At the spreading level, the concentration of particles is typi-

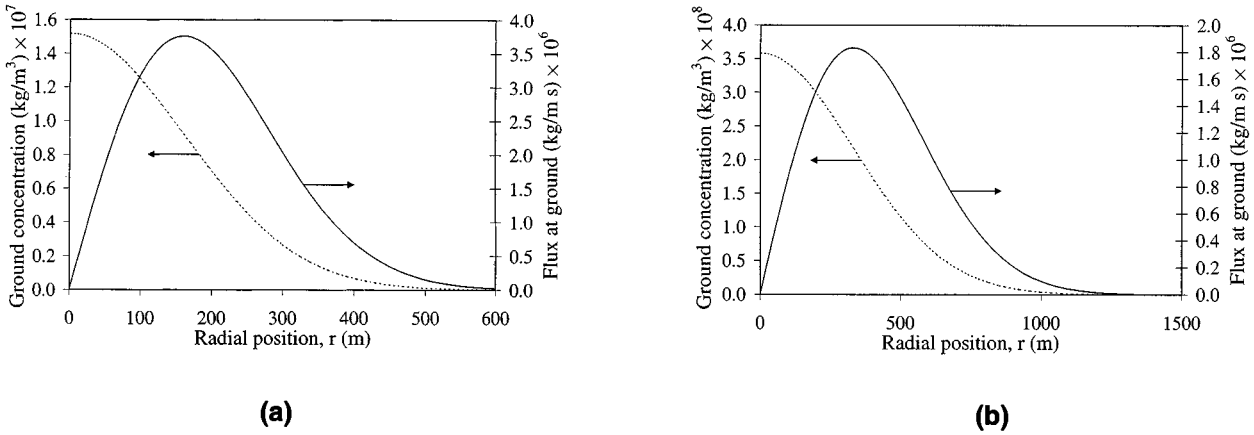

Figure 10. Theoretical predictions for the flux and concentration of particles at ground level for typical emissions of ash particles from (a) a boiler and (b) a combined gas turbine plant.

cally a few hundred times smaller than that at the source. Ash particles of diameter 30 μm can be transported to distances of up to 1,000 m from the source, at ground level. For an emission with a particulate concentration of 4×10^{-5} kg/m^3, the maximum concentration of particles at the ground level is of the order of 1×10^{-7} kg/m^3 and occurs near the source. Our theoretical treatment is general and should be applicable to other forms of buoyant particle-laden flows, found both in industry and in nature.

Literature Cited

Allen, T., *Particle Size Measurement*, Chapman and Hall, London, U.K. (1997).

Baines, W. D., and J. S. Turner, ''Turbulent Buoyant Convection from a Source in a Confined Region,'' *J. Fluid Mech.*, **37**, 31 (1969).

Benet, N., L. Falk, H. Muhr, and E. Plasari, ''Experimental Study of a Two-Impinging-Jet Device for Application in Precipitation Process,'' *Proc. 14th Int. Symp. on Ind. Crystallisation*, Cambridge, U.K. (1999).

Briggs, G. A., *Plume Rise*, U.S. Atomic Energy Commission Critical Review Series (1969).

Carey, S. N., H. Sigurdsson, and R. S. J. Sparks, ''Experimental Studies of Particle-Laden Plumes,'' *J. Geophys. Res.*, **93**, 15, 314 (1988).

Ernst, G. J., R. S. J. Sparks, S. N. Carey, and M. I. Bursik, ''Sedimentation from Turbulent Jets and Plumes,'' *J. Geophys. Res.*, **101**, 5575 (1996).

Feely, R., M. Lewison, G. Massoth, G. Robert-Baldo, J. Lavelle, R. Byrne, K. Van Damm, and H. Curl, ''Composition and Dissolution of Black Smoker Particulates from Active Vents on the Juan de Fuca Ridge,'' *J. Geophys. Res.*, **92**, 11, 347 (1987).

List, E. J., ''Turbulent Jets and Plumes,'' *Annu. Rev. Fluid Mech.*, **14**, 189 (1982).

Martin, D., and R. Nokes, ''Crystal Settling in a Convecting Magma Chamber,'' *Nature*, **332**, 534 (1988).

Manins, P. C., ''Confined Convective Flows,'' PhD Thesis, University of Cambridge, U.K. (1973).

Manins, P. C., ''Turbulent Buoyant Convection from a Source in a Confined Region,'' *J. of Fluid Mech.*, **91**, 765 (1979).

Morton, B. R., F. R. S. Taylor, and J. S. Turner, ''Turbulent Gravitational Convection from Maintained and Instantaneous Sources,'' *Proc. Roy. Soc. A.*, **234**, 1 (1956).

Papanicolaou, P. N., and E. J. List, ''Investigations of Round Vertical Turbulent Buoyant Jets,'' *J. of Fluid Mech.*, **195**, 341 (1988).

Schaflinger, U., T. Aihara, T. Gruber, U. Weingerl, T. Ohara, and W. Schneider, ''Analysis of Particle Motion in a Very Shallow Fluidized Bed,'' *Int. J. Multiphase Flow*, **23**, 455 (1997).

Sparks, R. S. J., S. N. Carey, and H. Sigurdson, ''Sedimentation from Gravity Currents Generated by Turbulent Plumes,'' *Sedimentology*, **38**, 856 (1991).

Staples, T., ''The Implications of 'New Generation' Gas Dispersion Models for Stack Heights and Pollution Abatement,'' *IChemE Environ. Bull.*, **047**, 13 (1997).

Tritton, D. J., *Physical Fluid Dynamics*, Oxford University Press, Oxford, U.K. (1988).

Turner, J. S., *Buoyancy Effects in Fluids*, Cambridge University Press, Cambridge, U.K. (1979).

Turner, J. S., ''Turbulent Entrainment—the Development of the Entrainment Assumption, and its Application to Geophysical Flows,'' *J. of Fluid Mech.*, **173**, 431 (1986).

Weast, R. C., *CRC Handbook of Chemistry and Physics*, 52nd ed., CRC Press, Boca Raton, FL (1971).

Manuscript received Sept. 24, 1999, and revision received June 23, 2000.